Materials Physics and Mechanics 9 (2010) 53-67 Received: March 17, 2010

MAGNETIC PROPERTIES OF Ni_2MnGa ALLOY

T. Breczko[1]*, V.V. Barkaline[2], R.M. Grechishkin[3], V.V. Nelayev[4]

[1] University of Bialystok, 64 Sosnowa str. 15-887 Bialystok, Poland

[2] Belarussian National Technical University, Nezavisimosti ave. 65, 220013 Minsk, Belarus

[3] Department of Physics, Tver State University, Zhelyabova str. 33, 170000 Tver, Russia

[4] Belarusian State University of Informatics and Radioelectronics, P. Brovki str. 6, 220013 Minsk, Belarus

* E-mail: tbreczko@uwb.edu.pl

Abstract. The paper presents results of the computer simulations and experimental investigation of physical properties of Ni-Mn-Ga alloy. The study was performed using atomic force microscope. The chemical composition of researched specimens causes generation of martensite and austenite phases. Computer simulations are devoted to austenite phase.

1. Introduction

Over the last decade, great progress has been seen in the development of smart structure technology. This is partly due to the fact that intelligent materials usable as functional components of smart structures have been extensively studied. Particularly in actuator technology, active or smart materials have opened new horizons in terms of actuation simplicity, compactness and miniaturization potential. Shape memory alloys (SMA's) are functional materials. Heusler Ni_2MnGa alloys belong to a class of materials known as ferromagnetic shape memory alloys which can change their length by up to 10% on application of a magnetic field. Combination of ferromagnetism and structural phase transitions in Heusler alloys is perspective for production of new devices based on the magnetic field control of the size and shape of the actuator active elements. The structural phase transitions in these elements proceed by the transformation of high-temperature austenite cubic phase into a tetragonal low-temperature martensite phase.

Ni-Mn-Ga alloys of the composition about stoichiometric phase Ni_2MnGa have at room temperature the face centered cubic Heusler's structure ($L2_1$, no. 225). Under cooling these alloys, the structural transition in the low temperature phase (martensite) proceeds. In this state compounds have some characteristic behaviour in an external magnetic field, i.e. macroscopic strain is obtained by martensite's twin boundary moving. For the first time this effect and its mechanism was described by Ullakko in 1996, and now it is intensively examined. In the stoichiometric compound, the magnetic field produced strain (MFPS) is about *0.2%*. Small modification in the atomic composition gives possibility to obtain strains up to 6% or even 10%. It depends on the martensite structure (tetragonal or orthorhombic). The crystallographic structure and the temperature interval of the existence of martensitic and austenitic phase are strongly depending on atomic composition. This property gives possibility to produce new kind of actuators based on magnetic shape memory (MSM) effect. This effect and related crystallographic structures are widely reported by Ullakko, Kokorin and Martynov. From the technological point of view alloys with MSM should have martensitic structure at room temperature and in wide range about it.

Detailed experimental studies of the regularities of formation and realignment of both martensitic and magnetic domain structure (DS) are necessary for modeling and simulation of magnetically induced phenomena in these alloys. These questions are studied intensively by a large number of research groups [1-9]. However the available data are still fragmentary and are needed to be extended and generalized. In the present work we focus our attention on martensite transformation and electron properties of Ni_2MnGa alloys.

2. Methodology and experiment

In our study we investigate the structure of Ni-Mn-Ga alloy after a casting and then after thermal annealing. A sample was obtained by arc-melt method in argon atmosphere. The sample was annealed at 1127K for the time 72h in argon atmosphere and was cooled in a furnace to room temperature. Chemical composition was defined with scanning electron microscope (SME) Vega TS 5135 MM Tescan provided with X-ray microanalyser – EXD ISIS Link 300 Oxford Instruments. The X-ray microanalysis has shown small value of standard deviation, by this means that the sample had homogenous composition. The results are given in Table1.

Table 1. Chemical composition of investigated Ni-Mn-Ga sample.

Ni		Mn		Ga	
at. %	standard dev.	at. %	standard dev.	at. %	standard dev.
56.48	0.2	18.12	0.3	25.39	0.22

Before observation the sample was polished mechanically with water paper and suspended Al_2O_3. The sample was chemically etched in solution containing $50ml(H_2O)+50ml(HCl)+10g(CuSO_4)$.

SFM investigation was taken with SFM type SMENA_B made by NT-MDT (Russia) in air at room temperature. Commercial long rectangle cantilever was used. SFM measurement was performed in contact regime. Cantilever's parameters are presented in Table 2.

Table 2. Properties of a cantilever.

Length [μm]	350
Width [μm]	35
Thickness [μm]	1.0
Force constant [N/m]	0.03
Resonant frequency [kHz]	10

Microstructure of the investigated alloy after cast without any stabilisation or homogenisation is shown in Fig. 1. The results indicate that the grain structure is irregular. But columnar structure of the grain morphology allow suggest that a twin structure can be obtained after thermal stability. Widely we reported this state earlier [10].

3. Simulation of atomic clusters in NWChem package

NWChem is a computational chemistry package that is designed to run on high-performance parallel supercomputers as well as conventional workstation clusters. It aims to be scalable both in its ability to treat large problems efficiently, and in its usage of available parallel computing resources. NWChem has been developed by the Molecular Sciences Software group of the Environmental Molecular Sciences Laboratory (EMSL) at the Pacific Northwest National Laboratory (PNNL), USA [11].

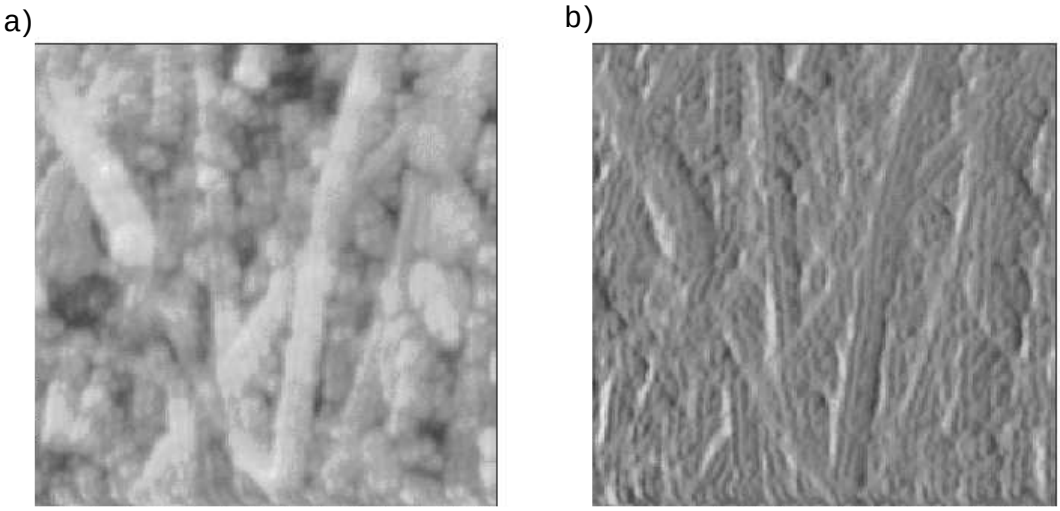

Fig. 1. SFM surface structure of Ni56.48Mn18.12Ga25.39 alloy after casting; scan area 14.5x14.5 μm.
a) Height signal, b) Lateral force signal.

Simulation of the influence of the atomic structure of magnetic alloys on their physical properties implies using *ab initio* quantum mechanical approaches. At present there are two distinct directions of computational materials science both dealing with ab initio calculation of material properties: the band structure calculations based on translation periodicity of the crystalline media and cluster calculations similar to the quantum chemistry approach. The results on the band structure calculation of electronic properties of magnetic shape-memory alloy Ni_2MnGa were presented earlier [12]. In the present paper we discuss the cluster approach to simulation of this material.

The cluster approach implies solving stationary Schrödinger equation for a small sample of a material considered as an isolated system of electrons and atomic nuclei with Coulomb interaction between them. At present clusters containing up to one hundred atoms can be considered by this way using a supercomputer. The ultimate goal of *ab initio* cluster calculations is the solution of the time-independent, non-relativistic Schrödinger equation

$$\mathbf{H}\Psi(\vec{r}_1,\sigma_1,\cdots,\vec{r}_L,\sigma_L,\vec{R}_1,\cdots,\vec{R}_M) = E\Psi(\vec{r}_1,\sigma_1,\cdots,\vec{r}_L,\sigma_L,\vec{R}_1,\cdots,\vec{R}_M) \quad (1)$$

where $\vec{r}_i,\sigma_i$ ($i=1,\ldots,L$) are the radius-vectors and the spin variables of cluster electrons, $\vec{R}_a$, ($a=1,\ldots, M$) are the radius-vectors of cluster nuclei, Ψ is the cluster wave function, E is the cluster energy. Hamilton operator of cluster is taken usually as

$$\mathbf{H} = \mathbf{T}_N + \mathbf{V}_N + \mathbf{H}_{N\mathbf{e}}; \quad (2)$$

where $\mathbf{T}_N$ is the operator of kinetic energy of nuclei, $\mathbf{V}_N$ is their Coulomb energy, $\mathbf{H}_{N\mathbf{e}}$ is the Hamilton operator of electrons in the field of nuclei.

Due to their large masses, the nuclei move much slower than the electrons and one can consider the electrons as moving in the field of fixed nuclei (adiabatic approach). Thus the nuclear kinetic energy is zero and their potential energy is merely a constant. This means that the electronic Hamiltonian reduces to

$$\mathbf{H}_{N\mathbf{e}} = \mathbf{T} + \mathbf{V}_{N\mathbf{e}} + \mathbf{V}_{\mathbf{ee}} \quad (3)$$

with components

$$\mathbf{T} = -\sum_{i=1}^{L} \frac{\hbar^2}{2m}\nabla_i^2; \quad (4)$$

$$\mathbf{V}_{Ne} = -\sum_{i=1}^{L}\sum_{a=1}^{M}\frac{Z_a e^2}{\left|\vec{r}_i - \vec{R}_a\right|}; \tag{5}$$

$$\mathbf{V}_{ee} = \sum_{i=1}^{L}\sum_{j<i}\frac{e^2}{\left|\vec{r}_i - \vec{r}_j\right|} \tag{6}$$

corresponding to the kinetic energy of electrons, their interaction with nuclei and between themselves, respectively. The full set of electronic Hamiltonian wave functions $\Phi_m(\vec{r}_1,\sigma_1,\cdots,\vec{r}_L,\sigma_L,\vec{R}_1,\cdots,\vec{R}_M)$, ($m=0,\ldots,\infty$), which are the solution of the eigenvalue problem

$$\mathbf{H}_{Ne}\Phi_m(\vec{r}_1,\sigma_1,\cdots,\vec{r}_L,\sigma_L,\vec{R}_1,\cdots,\vec{R}_M) = E_m(\vec{R}_1,\cdots,\vec{R}_M)\Phi_m(\vec{r}_1,\sigma_1,\cdots,\vec{r}_L,\sigma_L,\vec{R}_1,\cdots,\vec{R}_M), \tag{7}$$

make it possible to represent every cluster wave function as the series

$$\Psi(\vec{r}_1,\sigma_1,\cdots,\vec{r}_L,\sigma_L,\vec{R}_1,\cdots,\vec{R}_M) = \sum_m \chi_m(\vec{R}_1,\cdots,\vec{R}_M)\Phi_m(\vec{r}_1,\sigma_1,\cdots,\vec{r}_L,\sigma_L,\vec{R}_1,\cdots,\vec{R}_M) \tag{8}$$

with the nuclei wave functions in m-th electronic state $\chi_m(\vec{R}_1,\cdots,\vec{R}_M)$. For the nuclei fixed at positions $\vec{R}_1^{(0)},\cdots,\vec{R}_M^{(0)}$

$$\chi_m(\vec{R}_1,\cdots,\vec{R}_M) = C_m\delta(\vec{R}_1 - \vec{R}_1^{(0)})\cdots\delta(\vec{R}_M - \vec{R}_M^{(0)}), \tag{9}$$

where $\delta(\vec{x})$ is Dirac δ-function.

Self consistent field approximation. The main problem in solving (7) is the electrons' interaction term $\mathbf{V}_{ee}$ in Hamiltonian (3) which makes it impossible to separate variables corresponding to different electrons and reduce multi-electron task to the set of L simplest one-electron tasks dealing with the movement of single electron in some external field – this means that electrons move in cluster correlatively. To get most accurate single-electron description of multi-electron system (orbital model), the electronic Hamiltonian is presented as

$$\mathbf{H}_{Ne} = \sum_{i=1}^{L}\left(\mathbf{h}_i + \left[\sum_{j\neq i}\frac{e^2}{\left|\vec{r}_i - \vec{r}_j\right|} - \mathbf{u}_i(\vec{r}_i)\right]\right) \tag{10}$$

where the single-electron Hamiltonian

$$\mathbf{h}_i = -\frac{\hbar^2}{2m}\nabla_i^2 - \sum_{a=1}^{M}\frac{Z_a e^2}{\left|\vec{r}_i - \vec{R}_a\right|} + \mathbf{u}_i(\vec{r}_i) \tag{11}$$

contains effective potential field $\mathbf{u}_i(\vec{r})$ which approximate the influence of all other electrons on the movement of electron i. Best possible choose of $\mathbf{u}_i(\vec{r})$ is obtained from self consistent field method and leads to Hartree-Fock approximation.

This approximation uses the full set of orthogonal normalized solutions of single-electron Schrödinger equation $\{\varphi_n(\vec{r},\sigma,\vec{R}_1,\cdots,\vec{R}_M)\}$,

$$\mathbf{h}_i\varphi_n(\vec{r}_i,\sigma_i,\vec{R}_1,\cdots,\vec{R}_M) = \varepsilon_n\varphi_n(\vec{r}_i,\sigma_i,\vec{R}_1,\cdots,\vec{R}_M) \tag{12}$$

corresponding to the eigenvalues ε_n, (n=0,…,∞), to represent L-electron wavefunction of cluster in Slater determinant form:

$$\Phi_L(\vec{r}_1,\sigma_1,..,\vec{r}_L,\sigma_L,\vec{R}_1,..,\vec{R}_M) = \frac{1}{\sqrt{L!}}\det\begin{bmatrix} \varphi_1(\vec{r}_1,\sigma_1;\vec{R}_1,\cdots,\vec{R}_M) & \cdots & \varphi_1(\vec{r}_L,\sigma_L;\vec{R}_1,\cdots,\vec{R}_M) \\ \varphi_2(\vec{r}_1,\sigma_1;\vec{R}_1,\cdots,\vec{R}_M) & \cdots & \varphi_2(\vec{r}_L,\sigma_L;\vec{R}_1,\cdots,\vec{R}_M) \\ \vdots & \vdots & \vdots \\ \varphi_L(\vec{r}_1,\sigma_1;\vec{R}_1,\cdots,\vec{R}_M) & \cdots & \varphi_L(\vec{r}_L,\sigma_L;\vec{R}_1,\cdots,\vec{R}_M) \end{bmatrix} \tag{13}$$

Every spin-orbital $\varphi_n(\vec{r},\sigma,\vec{R}_1,\cdots,\vec{R}_M)$ from (13) can be represented as the product of spatial orbital $\psi_n(\vec{r},\vec{R}_1,\cdots,\vec{R}_M)$ and one of two spin functions $\alpha(\sigma)$ or $\beta(\sigma)$ corresponding to two possible spin projection values of an electron.

Expectation value of the electronic Hamiltonian $\mathbf{H}_{Ne}$ in Φ_L state can be represented as

$$E_{HF}(\vec{R}_1,\cdots,\vec{R}_M)=\frac{\langle\Phi_L|\mathbf{H}_{Ne}|\Phi_L\rangle}{\langle\Phi_L|\Phi_L\rangle} \tag{14}$$

and for wave function (13) can be represented as

$$E_{HF}(\vec{R}_1,\cdots,\vec{R}_M)=\sum_{i=1}^{L}E_i(\vec{R}_1,\cdots,\vec{R}_M)+\frac{1}{2}\sum_{i,j=1}^{L}\left(J_{ij}(\vec{R}_1,\cdots,\vec{R}_M)-K_{ij}(\vec{R}_1,\cdots,\vec{R}_M)\right), \tag{15}$$

where one-electron energies E_i, Coulomb integrals J_{ij} and exchange integrals K_{ij} all are non-negative and defined as follows:

$$E_i=\sum_{\sigma}\int d\vec{r}\,\overline{\varphi}_i(\vec{r},\sigma,\vec{R}_1,\cdots,\vec{R}_M)\left(-\frac{\hbar^2}{2m}\nabla^2-\sum_{a=1}^{M}\frac{Z_a e^2}{|\vec{r}-\vec{R}_a|}\right)\varphi_i(\vec{r},\sigma,\vec{R}_1,\cdots,\vec{R}_M), \tag{16}$$

$$\begin{aligned}J_{ij}=&\sum_{\sigma_1\sigma_2}\int\int d\vec{r}_1 d\vec{r}_2\,\overline{\varphi}_i(\vec{r}_1,\sigma_1,\vec{R}_1,\cdots,\vec{R}_M)\times\\&\varphi_i(\vec{r}_1,\sigma_1,\vec{R}_1,\cdots,\vec{R}_M)\frac{e^2}{|\vec{r}_1-\vec{r}_2|}\overline{\varphi}_j(\vec{r}_2,\sigma_2,\vec{R}_1,\cdots,\vec{R}_M)\varphi_j(\vec{r}_2,\sigma_2,\vec{R}_1,\cdots,\vec{R}_M),\end{aligned} \tag{17}$$

$$\begin{aligned}K_{ij}=&\sum_{\sigma_1\sigma_2}\int\int d\vec{r}_1 d\vec{r}_2\,\overline{\varphi}_i(\vec{r}_1,\sigma_1,\vec{R}_1,\cdots,\vec{R}_M)\times\\&\varphi_j(\vec{r}_1,\sigma_1,\vec{R}_1,\cdots,\vec{R}_M)\frac{e^2}{|\vec{r}_1-\vec{r}_2|}\overline{\varphi}_j(\vec{r}_2,\sigma_2,\vec{R}_1,\cdots,\vec{R}_M)\varphi_i(\vec{r}_2,\sigma_2,\vec{R}_1,\cdots,\vec{R}_M).\end{aligned} \tag{18}$$

Obviously $J_{ii}=K_{ii}$.

Equations (16)-(18) show that for a fixed set of spin-orbitals contributing to $\Phi_L(\vec{r}_1,\sigma_1,\cdots,\vec{r}_L,\sigma_L,\vec{R}_1,\cdots,\vec{R}_M)$ the most adequate choose of the effective potential $\mathbf{u}_i(\vec{r})$ is

$$\mathbf{u}_i(\vec{r})=\sum_{j=1}^{L}(\mathbf{J}_j(\vec{r})-\mathbf{K}_j(\vec{r})) \tag{19}$$

with Coulomb **J** and exchange **K** operators acting on the spin-orbitals in accordance with the relationships

$$\mathbf{J}_j(\vec{r})\varphi_i(\vec{r},\sigma,\vec{R}_1,\cdots,\vec{R}_M)=\sum_{\sigma_1}\int d\vec{r}_1\left|\varphi_j(\vec{r}_1,\sigma_1,\vec{R}_1,\cdots,\vec{R}_M)\right|^2\frac{e^2}{|\vec{r}-\vec{r}_1|}\cdot\varphi_i(\vec{r},\sigma,\vec{R}_1,\cdots,\vec{R}_M) \tag{20}$$

$$\begin{aligned}&\mathbf{K}_j(\vec{r})\varphi_i(\vec{r},\sigma,\vec{R}_1,\cdots,\vec{R}_M)=\\&=\sum_{\sigma_1}\int d\vec{r}_1\overline{\varphi}_j(\vec{r}_1,\sigma_1,\vec{R}_1,\cdots,\vec{R}_M)\varphi_i(\vec{r}_1,\sigma_1,\vec{R}_1,\cdots,\vec{R}_M)\frac{e^2}{|\vec{r}-\vec{r}_1|}\cdot\varphi_j(\vec{r},\sigma,\vec{R}_1,\cdots,\vec{R}_M)\end{aligned} \tag{21}$$

Such defined potential is named Hartree-Fock potential, it is non-local and depends on the spin-orbitals. The Koopman's theorem provides a physical interpretation of the orbital energies: it states that the orbital energy ε_i is an approximation of the ionization energy associated with the removal of an electron from the orbital φ_i.

Because of orbital dependence of Hartree-Fock potential, the orbitals themselves must be defined in a self-consistent manner. A trial set of spin-orbitals is formulated and used to

construct the Fock operator (11), where (18) is used for $\mathbf{u}_i(\vec{r})$, then the equations (12) are solved to obtain a new set of spin-orbitals that are used to construct a revised Fock operator, and so on. The cycle of calculation and reformulation is repeated until a convergence criterion is satisfied. Such obtained spin-orbitals realize stationary point of energy (15) as functional of spin-orbitals (the latter are assumed to be orthonormal).

In self-consistent field calculations on closed-shell states of atomic clusters with even number of electrons, it is supposed that the spatial parts of the spin-orbitals are identical for electrons of every electron pair. There are then L/2 spatial orbitals of the form $\psi_n(\vec{r},\vec{R}_1,\cdots,\vec{R}_M)$ and the L-electron wavefunction is

$$\Phi_{RHF}(\vec{r}_1,\sigma_1,..,\vec{r}_L,\sigma_L,\vec{R}_1,..,\vec{R}_M) = \frac{1}{\sqrt{L!}}\det\begin{bmatrix} \psi_1(\vec{r}_1,\vec{R}_1,\cdots,\vec{R}_M)\alpha(\sigma_1) & \cdots & \psi_1(\vec{r}_L,\vec{R}_1,\cdots,\vec{R}_M)\alpha(\sigma_L) \\ \psi_1(\vec{r}_1,\vec{R}_1,\cdots,\vec{R}_M)\beta(\sigma_1) & \cdots & \psi_1(\vec{r}_L,\vec{R}_1,\cdots,\vec{R}_M)\beta(\sigma_L) \\ \psi_2(\vec{r}_1,\vec{R}_1,\cdots,\vec{R}_M)\alpha(\sigma_1) & \cdots & \psi_2(\vec{r}_L,\vec{R}_1,\cdots,\vec{R}_M)\alpha(\sigma_L) \\ \vdots & \vdots & \vdots \\ \psi_{L/2}(\vec{r}_1,\vec{R}_1,\cdots,\vec{R}_M)\beta(\sigma_1) & \cdots & \psi_{L/2}(\vec{r}_L,\vec{R}_1,\cdots,\vec{R}_M)\beta(\sigma_L) \end{bmatrix}. \quad (22)$$

Such a wave function is called a restricted Hartree-Fock (RHF) wavefunction.

For open-shell states of atomic clusters two approaches are commonly used. In the restricted open-shell formalism (ROHF), all electrons, except those occupying m open-shell orbitals, are forced to occupy doubly occupied (L-m)/2 spatial orbitals:

$$\Phi_{ROHF}(\vec{r}_1,\sigma_1,..,\vec{r}_L,\sigma_L,\vec{R}_1,..,\vec{R}_M) = \frac{1}{\sqrt{L!}}\det\begin{bmatrix} \psi_1(\vec{r}_1,\vec{R}_1,\cdots,\vec{R}_M)\alpha(\sigma_1) & \cdots & \psi_1(\vec{r}_L,\vec{R}_1,\cdots,\vec{R}_M)\alpha(\sigma_L) \\ \vdots & \vdots & \vdots \\ \psi_m(\vec{r}_1,\vec{R}_1,\cdots,\vec{R}_M)\alpha(\sigma_1) & \cdots & \psi_m(\vec{r}_L,\vec{R}_1,\cdots,\vec{R}_M)\alpha(\sigma_L) \\ \psi_{m+1}(\vec{r}_1,\vec{R}_1,\cdots,\vec{R}_M)\alpha(\sigma_1) & \cdots & \psi_{m+1}(\vec{r}_L,\vec{R}_1,\cdots,\vec{R}_M)\alpha(\sigma_L) \\ \psi_{m+1}(\vec{r}_1,\vec{R}_1,\cdots,\vec{R}_M)\beta(\sigma_1) & \cdots & \psi_{m+1}(\vec{r}_L,\vec{R}_1,\cdots,\vec{R}_M)\beta(\sigma_L) \\ \vdots & \vdots & \vdots \\ \psi_{(L-m)/2}(\vec{r}_1,\vec{R}_1,\cdots,\vec{R}_M)\beta(\sigma_1) & \cdots & \psi_{(L-m)/2}(\vec{r}_L,\vec{R}_1,\cdots,\vec{R}_M)\beta(\sigma_L) \end{bmatrix}. \quad (23)$$

In the unrestricted open-shell Hartree-Fock (UHF) formalism any two electrons are not constrained to the same spatial wave function and L-electron wave function has the general form (13). By relaxing the constraint of occupying orbitals in pairs, the open-shell UHF formalism gives a lower variational energy than the ROHF formalism. However, one disadvantage of the UHF approach is that whereas the RHF and ROHF wave functions are the eigenfunctions of the total cluster spin operator, the UHF function is not; that is, the total spin angular momentum is not well-defined for the UHF wavefunction.

In practical calculations cluster spatial orbitals are expanded into a finite series of $K \geq L$ basis functions $\xi_k(\vec{r},\vec{R}_1,\cdots\vec{R}_M)$:

$$\psi_i(\vec{r},\vec{R}_1,\cdots,\vec{R}_M) = \sum_{k=1}^{K} C_{ki}(\vec{R}_1,\cdots\vec{R}_M)\xi_k(\vec{r},\vec{R}_1,\cdots\vec{R}_M). \quad (24)$$

It is useful to introduce vector and matrix notation for orbitals

$$\boldsymbol{\psi} = \{\psi_1,\cdots,\psi_L\};\quad \boldsymbol{\xi} = \{\xi_1,\cdots,\xi_K\};\ \mathbf{C} = \{C_{ki}\}. \quad (25)$$

Then, equation (24) can be rewritten as

$$\boldsymbol{\psi} = \mathbf{C}\boldsymbol{\xi}. \quad (26)$$

Then for closed shell RHF formalism energy relation (15) can be transformed to

$$E_{HF}(\vec{R}_1,\cdots,\vec{R}_M) = Sp\{\mathbf{R}(\mathbf{h}+\frac{1}{2}\mathbf{G})\}\,, \tag{27}$$

where $\mathbf{R} = \mathbf{C}\mathbf{C}^+$, $\mathbf{G} = 2\mathbf{J} - \mathbf{K}$,

$$\mathbf{h}_{ij} = \int d\vec{r}\,\overline{\xi}_i(\vec{r},\vec{R}_1,\cdots,\vec{R}_M)\left(-\frac{\hbar^2}{2m}\nabla^2 - \sum_{a=1}^{M}\frac{Z_a e^2}{\left|\vec{r}-\vec{R}_a\right|}\right)\xi_j(\vec{r},\vec{R}_1,\cdots,\vec{R}_M)\,, \tag{28}$$

$$\begin{aligned}\mathbf{J}_{ij} = \sum_{p,q=1}^{K}\mathbf{R}_{pq}\int\int d\vec{r}_1 d\vec{r}_2\,\overline{\xi}_i(\vec{r}_1,\vec{R}_1,\cdots,\vec{R}_M)\times \\ \xi_j(\vec{r}_1,\vec{R}_1,\cdots,\vec{R}_M)\frac{e^2}{\left|\vec{r}_1-\vec{r}_2\right|}\overline{\xi}_q(\vec{r}_2,\vec{R}_1,\cdots,\vec{R}_M)\xi_p(\vec{r}_2,\vec{R}_1,\cdots,\vec{R}_M),\end{aligned} \tag{29}$$

$$\begin{aligned}\mathbf{K}_{ij} = \sum_{p,q=1}^{K}\mathbf{R}_{pq}\int\int d\vec{r}_1 d\vec{r}_2\,\overline{\xi}_i(\vec{r}_1,\vec{R}_1,\cdots,\vec{R}_M)\times \\ \xi_p(\vec{r}_1,\vec{R}_1,\cdots,\vec{R}_M)\frac{e^2}{\left|\vec{r}_1-\vec{r}_2\right|}\overline{\xi}_q(\vec{r}_2,\vec{R}_1,\cdots,\vec{R}_M)\xi_j(\vec{r}_2,\vec{R}_1,\cdots,\vec{R}_M).\end{aligned} \tag{30}$$

If one introduces overlap matrix for the basis set orbitals $\mathbf{S}_{ij} = \int d\vec{r}\,\overline{\xi}_i(\vec{r},\vec{R}_1,\cdots,\vec{R}_M)\,\xi_j(\vec{r},\vec{R}_1,\cdots,\vec{R}_M)$, the necessary and sufficient condition of orthonormality for cluster orbitals can be represented as

$$\mathbf{RSR} = \mathbf{R}\,. \tag{31}$$

The stationarity condition for Hartree-Fock energy (27) accounting the orthonormality of the orbitals leads to Hartree-Fock matrix equations

$$(\mathbf{h}+\mathbf{G})\mathbf{C} = \mathbf{SC}\boldsymbol{\varepsilon}\,, \tag{32}$$

where $\boldsymbol{\varepsilon}$ is $L\times L$ matrix of Lagrange multipliers which can be chosen as a diagonal matrix with elements associated with the energies of corresponding cluster orbital.

Similarly can be treated the case of open shells, with some sophistication of definition of $\mathbf{G}$ and $\mathbf{C}$ matrixes.

Density functional theory. An alternative to the HF methods is the density functional theory (DFT). DFT begins not with the multi-electron wavefunction $\Phi(\vec{r}_1,\sigma_1,\cdots,\vec{r}_L,\sigma_L,\vec{R}_1,\cdots\vec{R}_M)$ and Schrödinger equation (7) but with the concept of the electron probability density, which is defined as the integral over the spin coordinates of all electrons and over all but one of the spatial variables

$$\rho(\vec{r}) = L\sum_{\sigma_1,\cdots,\sigma_L}\int\cdots\int d\vec{r}_2\cdots d\vec{r}_L\,\overline{\Phi}(\vec{r},\sigma_1,\cdots,\vec{r}_L,\sigma_L,\vec{R}_1,\cdots,\vec{R}_M)\Phi(\vec{r},\sigma_1,\cdots,\vec{r}_L,\sigma_L,\vec{R}_1,\cdots,\vec{R}_M) \tag{33}$$

This function determines the probability of finding any of the L electrons within a volume element $d\vec{r}$. The reason for the popularity of DFT is that it takes into account electron correlation. It can be used to do calculations on clusters of 100 or more atoms in significantly less time than HF methods. Integration of $\rho(\vec{r})$ over whole space gives the number of electrons in a cluster:

$$\int d\vec{r}\,\rho(\vec{r}) = L\,. \tag{34}$$

Major points of DFT theory is two Hohenberg-Kohn theorems. The first one demonstrates that the electron density uniquely determines the Hamiltonian operator and thus all the properties of the system. This theorem states that the external potential $\mathbf{V}_{Ne}(\vec{r})$ is (to within a constant) a unique functional of $\rho(\vec{r})$. Since, in its turn $\mathbf{V}_{Ne}(\vec{r})$ fixes $\mathbf{H}_{Ne}$, we see

that the full many particle ground state is a unique functional of $\rho(\vec{r})$. Thus, $\rho(\vec{r})$ determines L and $\mathbf{V}_{N\mathbf{e}}(\vec{r})$ and hence all the properties of the ground state, for example the kinetic energy $T[\rho]$, the potential energy of electron-nuclei interaction $V_{N\mathbf{e}}[\rho]$, the potential energy of electron-electron interactions $V_{\mathbf{ee}}[\rho]$ and the total electron energy $E_{N\mathbf{e}}[\rho]$, which can be written as

$$E_{N\mathbf{e}}[\rho] = T[\rho] + V_{N\mathbf{e}}[\rho] + V_{\mathbf{ee}}[\rho] = \int d\vec{r}\rho(\vec{r})\mathbf{V}_{N\mathbf{e}}(\vec{r}) + F_{HK}[\rho], \tag{35}$$

$$F_{HK}[\rho] = T[\rho] + V_{\mathbf{ee}}[\rho]. \tag{36}$$

The second Hohenberg-Kohn theorem states that the functional $F_{HK}[\rho]$, that delivers the ground state energy of the system, delivers the lowest energy if and only if the input density is the true ground state density. In other words this means that for any trial density $\tilde{\rho}(\vec{r})$, which satisfies the necessary boundary conditions such as $\tilde{\rho}(\vec{r}) \geq 0$, $\int d\vec{r}\tilde{\rho}(\vec{r}) = L$, and which is associated with some external potential $\mathbf{V}_{N\mathbf{e}}(\vec{r})$, the energy obtained from functional (35) represents an upper bound to the true ground state energy E_0. E_0 results if and only if the exact ground state density $\rho(\vec{r})$ is inserted in (35).

From $V_{\mathbf{ee}}[\rho]$ one can extract classical part $J[\rho]$,

$$V_{\mathbf{ee}}[\rho] = \frac{1}{2}\int\int d\vec{r}_1 d\vec{r}_2 \frac{e^2}{|\vec{r}_1 - \vec{r}_2|}\rho(\vec{r}_1)\rho(\vec{r}_2) + V_{ncl}[\rho] = J[\rho] + V_{ncl}[\rho]. \tag{37}$$

$V_{ncl}[\rho]$ is the non-classical contribution to the electron-electron interaction: self-interaction correction, exchange and Coulomb correlation.

The explicit form of the functionals $T[\rho]$ and $V_{ncl}[\rho]$ is the major task of DFT. To relate them to the well-known results of Hartree-Fock orbital theory the reference system of L non-interacting electrons with the same electron density function is introduced, for which the set of orthonormal spatial orbitals $\{\psi_i(\vec{r})\}, i = 1, \cdots, L$ defines

$$\rho_{ref}(\vec{r}) = \sum_{i=1}^{L} |\psi_i(\vec{r})|^2 = \rho(\vec{r}), \tag{38}$$

$$T_{ref} = \int d\vec{r}\,\overline{\psi}_i(\vec{r})\left(-\frac{\hbar^2}{2m}\nabla^2\right)\psi_i(\vec{r}) \neq T[\rho]. \tag{39}$$

Then if one combines all unknown contributions into one energy term $E_{XC}[\rho]$,

$$E_{XC}[\rho] = (T[\rho] - T_{ref}[\rho]) + (V_{\mathbf{ee}}[\rho] - J[\rho]), \tag{40}$$

the functional of cluster energy can be represented as

$$E_{N\mathbf{e}}[\rho] = T_{ref}[\rho] + V_{N\mathbf{e}}[\rho] + J[\rho] + E_{XC}[\rho] =$$
$$-\frac{\hbar^2}{2m}\int d\vec{r}\,\overline{\psi}_i(\vec{r})\nabla^2\psi_i(\vec{r}) - \sum_{i=1}^{L}\sum_{a=1}^{M}\int d\vec{r}\frac{Z_a e^2}{|\vec{r} - \vec{R}_a|} + \tag{41}$$
$$\frac{1}{2}\sum_{i=1}^{L}\sum_{j=1}^{L}\int\int d\vec{r}_1 d\vec{r}_2 |\psi_i(\vec{r}_1)|^2 \frac{e^2}{|\vec{r}_1 - \vec{r}_2|}|\psi_j(\vec{r}_1)|^2 + E_{XC}[\rho].$$

The only term for which no explicit form can be given is $E_{XC}[\rho]$. One now can apply the variational principle to answer the question about what condition must the orbitals $\psi_i(\vec{r})$ fulfill in order to minimize the energy expression (41) under the usual constraint $\int d\vec{r}\,\overline{\psi}_i(\vec{r})\psi_j(\vec{r}) = \delta_{ij}$. The resulting equations are the Kohn- Sham equations:

$$\left(-\frac{\hbar^2}{2m}\nabla^2 + V_{KS}(\vec{r})\right)\psi_i(\vec{r}) = \varepsilon_i\psi_i(\vec{r}), \tag{42}$$

where

$$V_{KS}(\vec{r}) = \int d\vec{r}_1 \frac{e^2}{\left|\vec{r}-\vec{r}_1\right|}\rho(\vec{r}_1) - \sum_{a=1}^{M}\frac{Z_a e^2}{\left|\vec{r}-\vec{R}_a\right|} + V_{XC}(\vec{r}) \tag{43}$$

and $V_{XC}(\vec{r}) = \delta E_{XC}[\rho]/\delta\rho$ is the variational derivative of exchange and correlation energy functional. The value of $V_{KS}(\vec{r})$ depends on the density, and therefore the Kohn-Sham equations have to be solved iteratively to obtain a self-consistent solution.

Most of the applications of the Kohn-Sham density functional theory make use of the linear combination of atomic orbitals (LCAO) expansion of the Kohn-Sham orbitals. Similarly to (24), in this approach one introduces a set of K predefined basis functions $\xi_k(\vec{r})$ and linearly expand the K-S orbitals as

$$\psi_i(\vec{r}) = \sum_{k=1}^{K} C_{ki}\xi_k(\vec{r}). \tag{44}$$

Basis functions for both SCF and DFT calculation usually are chosen among three possibilities:

I. *Slater-type-orbitals* (STO): they seem to be the natural choice for basis functions. They are exponential functions that mimic the exact eigenfunctions of a hydrogen atom. A typical STO is expressed as

$$\xi^{STO} = N\, r^{n-1}\, e^{-\beta r}\, Y_{lm}(\theta,\varphi). \tag{45}$$

Here n corresponds to the principal quantum number, the orbital exponent is termed β and $Y_{lm}(\theta,\varphi)$ are the usual spherical harmonics. Unfortunately, it is very difficult to compute many-center integrals with STO basis, and they do not play a major role in ordinary quantum chemistry.

II. *Gaussian-type-orbitals* (GTO). They have the following general form:

$$\xi^{GTO} = N\, x^l\, y^m\, z^n e^{-\alpha r^2}. \tag{46}$$

N is a normalization factor, α represents the orbital exponent. $J = l+m+n$ is used to classify the GTO as s-functions ($J=0$), p-functions ($J=1$), etc.

III. *Contracted Gaussian functions* (CGF) basis sets, in which several Gaussian functions are combined in a fixed linear combination:

$$\xi_i^{CGF} = \sum_{a=1}^{A} d_{ai}\xi_a^{GTO}. \tag{47}$$

A variety of exchange-correlation functionals, having names such as mPWPW91, B3LYP, MPW1K, PBE1PBE, BLYP, BP91, and PBE, have been developed for use in DFT calculations; the names designate a particular pairing of an exchange functional and a correlation functional. For example, BLYP functional is a combination of the gradient-corrected exchange functional developed by A.D. Becke and the gradient-corrected correlation functional developed by C. Lee, W. Yang, and R.G. Parr. Some of the functionals, such as B3LYP, represent hybrid DFT calculations that use Hartree-Fock corrections in conjunction with density functional correlation and exchange

Density functional theory has also been applied to study open-shell atoms and molecules on the basis of spin density concept. The spin density refers to the difference between the spin-up electron density and the spin-down electron density, and the exchange-correlation energy depends on the spin density as well as the total electron density. Namely such

approach has to be used in DFT investigations of the magnetic structures of metals and alloys.

The original density functional theory has been generalized to deal with many different situations: spin polarized systems, multicomponent systems such as nuclei and electron hole droplets, free energy at finite temperatures, superconductors with electronic pairing mechanisms, relativistic electrons, time-dependent phenomena and excited states, bosons, molecular dynamics, etc. The computation time required for a DFT calculation formally scales as the third power of the number of basis functions; as a result, DFT methods are computationally more efficient (though not necessarily more accurate) than HF-based formalisms, which scale as the fourth power of the number of basis functions.

4. Computer simulations results and discussion

Ni2MnGa Heusler alloys (HA) has a theoretical lattice constant of 5.811 Å (10.981 a.u.) and 5.729 Å (10.826 a.u.) for the ferromagnetic and the paramagnetic phase, respectively. The crystal structure of Ni2MnGa HA can be considered as a bcc-based fcc crystal with a chain of Ni-Mn-Ni-Ga along the <111> direction. In present paper simulations deal with the simplest structure unit of the material – the cluster containing 9 atoms which is presented in Fig. 2. We calculate electronic structure of this cluster by open shell restricted Hartree-Fock method (ROHF), by unrestricted Hartree-Fock method and density functional theory (DFT) using NWChem package [11]1. All calculations deal with the system of 252 electrons.

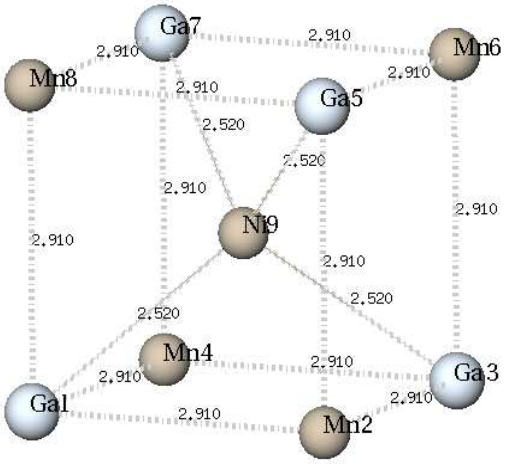

Fig. 2. Atomic structure of cluster $NiMn_4Ga_4$, the constitutive element of $L2_1$ cubic form of Ni_2MnGa.

Basis sets used in calculations are presented in Table 3. In all cases 6-31G* was used to represent atomic orbitals of Ni and Mn, and 6-311G** for Ga atoms in ROHF calculations. For DFT calculations the simplest 3-21G basis set for Ga was used. Contracted Gaussian functions (47) are used to represent atomic orbitals of every included electronic shell.

In Table 4 the SCF calculation results for energy components of cluster $NiMn_4Ga_4$ with various numbers of open shells with maximal value of total spin for ROHF and indefinite total spin for UHF calculations are presented. The similar results for DFT calculations are given in Table 5. Total energy for the last case is essentially larger then for the first one. This can be related to smaller basis set used for Ga atoms in DFT calculations.

In Fig. 3 the histogram of energy spectrum of the cluster is presented. The spectrum was calculated by RHF method for singlet closed shall state and ROHF and UHF methods for triplet, quintet and septet open shell states. In NWChem package, ROHF method is realized in such a way that only state with definite maximal spin is calculated. This means that all

electrons on single occupied shells have the same spin projection. For UHF method, term singlet is used for state with equal number of α- and β-electrons, triplet – for state with the number of α-electrons greater on 2 then that of β-electrons, quintet – for state with 4 excess α-electrons etc. Energy spectrum spin dependence for ROHF calculations is presented in Fig. 4, and it does not seem very strong.

Table 3. Characteristics of basis sets.

Atom	Atomic mass	Electronic configuration	Basis set	Number of shells	Number of Gaussian functions	Type of Gaussian functions
Ni	57.935300	$[Ar]3d^8 4s^2$	6-31G**	12	39	5s4p2d1f
Mn	54.938100	$[Ar]3d^5 4s^2$	6-31G**	12	39	5s4p2d1f
Ga	68.925700	$[Ar]3d^{10} 4s^2 4p^1$	6-311G**	18	47	8s7p3d
			3-21G	10	24	5s4p1d

Table 4. SCF calculated energy data in hartrees.

Parameter	Singlet	Calcula-tion type	Triplet	Quintet	Septet
Total SCF energy	-13797.099	ROHF	-13797.192	-13797.200	-13797.240
		UHF	-13797.636	-13797.741	-13797.891
One-electron energy	-28302.398	ROHF	-28299.751	-28293.491	-28293.438
		UHF	-28279.774	-28286.714	-28288.480
Two-electron energy	9948.029	ROHF	9945.288	9939.022	9938.927
		UHF	9924.868	9931.702	9933.318
Nuclear repulsion energy	4557.270	all	4557.270	4557.270	4557.270

Table 5. DFT calculated energy data in hartrees.

Parameter	Singlet	Triplet	Quintet	Septet
Total energy	-13774.816	-13775.206	-13775.140	-13775.258
Coulomb energy	10495.345	10494.026	10494.696	10493.838
Exchange energy	-573.100	-573.719	-573.618	-573.770
Nuclear repulsion energy	4557.270	4557.270	4557.270	4557.270

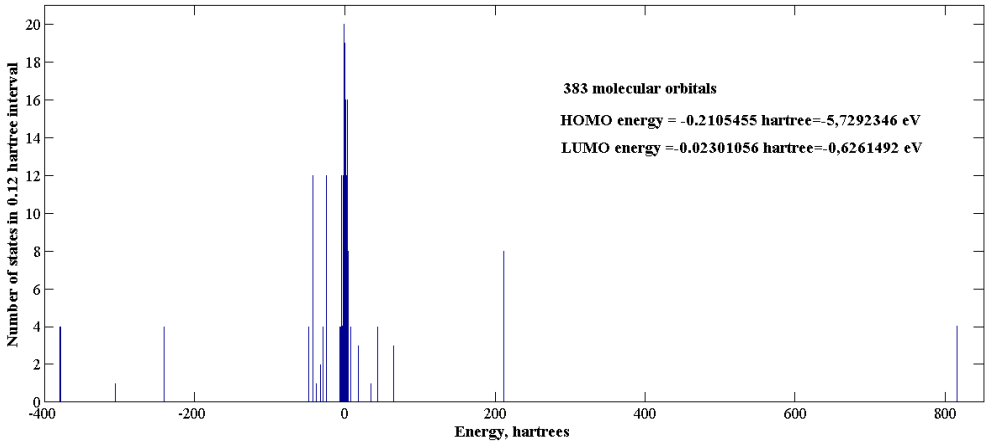

Fig. 3. Histogram of $NiMn_4Ga_4$ cluster energy spectrum with discretization 0.12 hartree. Common number of levels 383, RHF calculation. 126 molecular orbitals are double occupied. Highest occupied and lowest unoccupied molecular orbitals' energies are inserted.

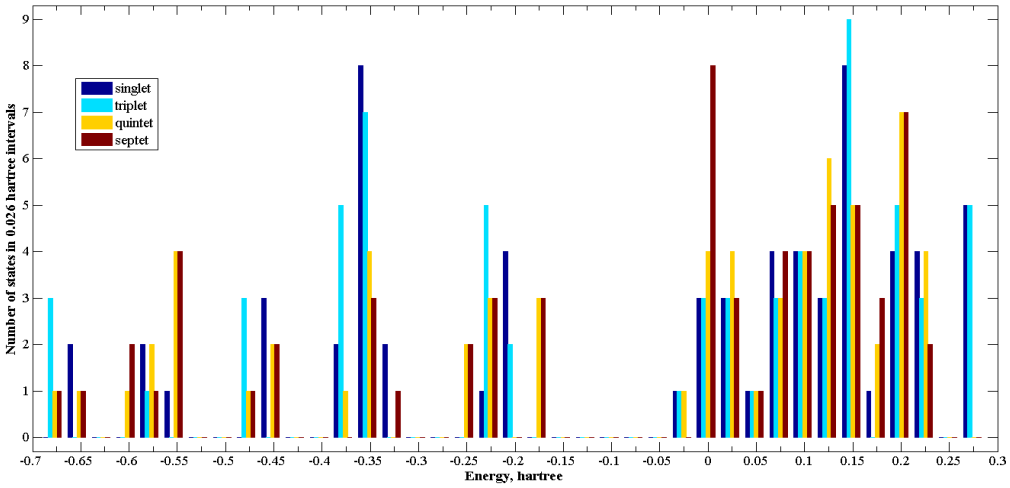

Fig. 4. Histogram of $NiMnm_4Ga_4$ cluster energy spectrum with discretization 0.026 hartree for various spin states from ROHF calculations near the HOMO and LUMO. Four neighbor lines correspond to the same interval.

Isosurfaces of electron density of the cluster in singlet state both for SCF and DFT calculations are presented in Fig. 5. The difference between the results is associated with d-electrons of Mn atoms of the cluster. For highest spin states a 'cubic' form of density near Mn atoms is present only for ROHF calculation. For UHF and DFT methods the results are very close for a given spin state. It is interesting that the form of isosurfaces very slightly depends on the spin state of cluster. For triplet and quintet states they are very similar to those presented in Fig. 6 for septet state.

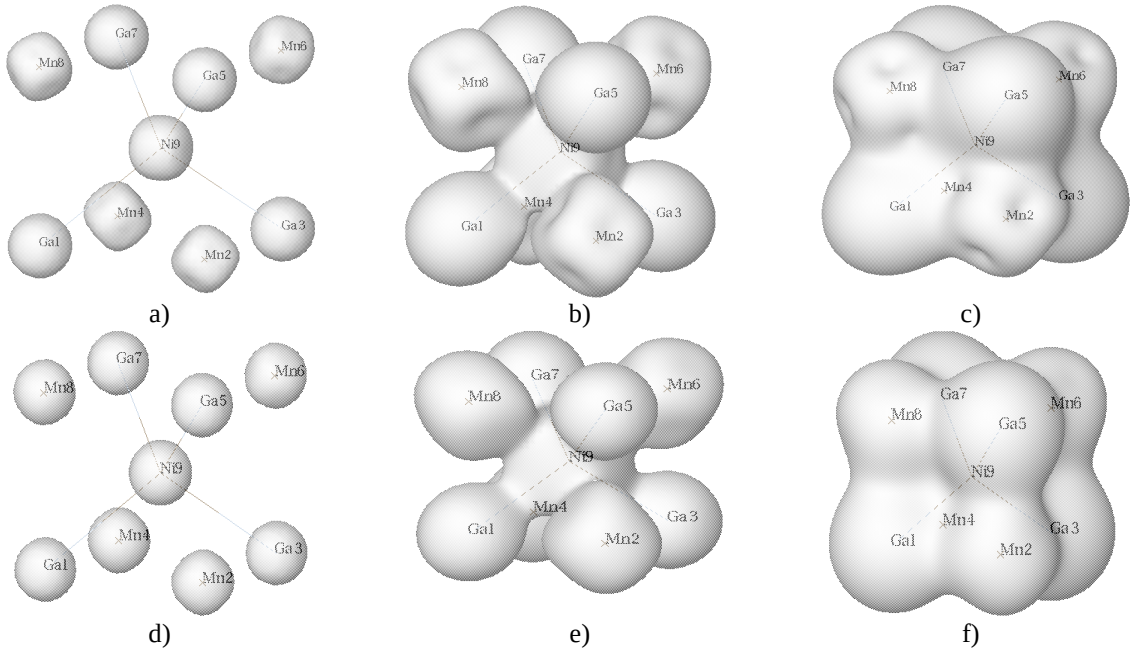

Fig. 5. Isosurfaces of electron density ρ for $NiMn_4Ga_4$ cluster in singlet state: a-c for RHF calculation, d-f for DFT calculation, a,d – isosurface corresponds to lg ρ=0; b,e – isosurface corresponds to lg ρ=-1.5; c,f - isosurface corresponds to lg ρ=-2.

Spin density studies show much less similarity of UHF and DFT calculations. For triplet state UHF calculation results in large spin density on Ga atoms which seems unseasonable. Clarifying this issue, one needs further investigation. Here we present only DFT results (Fig. 7). They show that Mn atoms play the main role in spin polarization of cluster and that this

role is played by different Mn atoms in different manner. Ni atom reduces the total polarization of the cluster because its negative contribution relatively the general contribution of Mn atoms. But the last is reduced partially by the 'clouds' of the negative spin density around the regions of positive one. This complex behavior of spin polarization in $NiMn_4Ga_4$ cluster promises interesting results for Ni_2MnGa cluster too. Such cluster of minimal size contains 35 atoms and for its study it is necessary to use supercomputer resources.

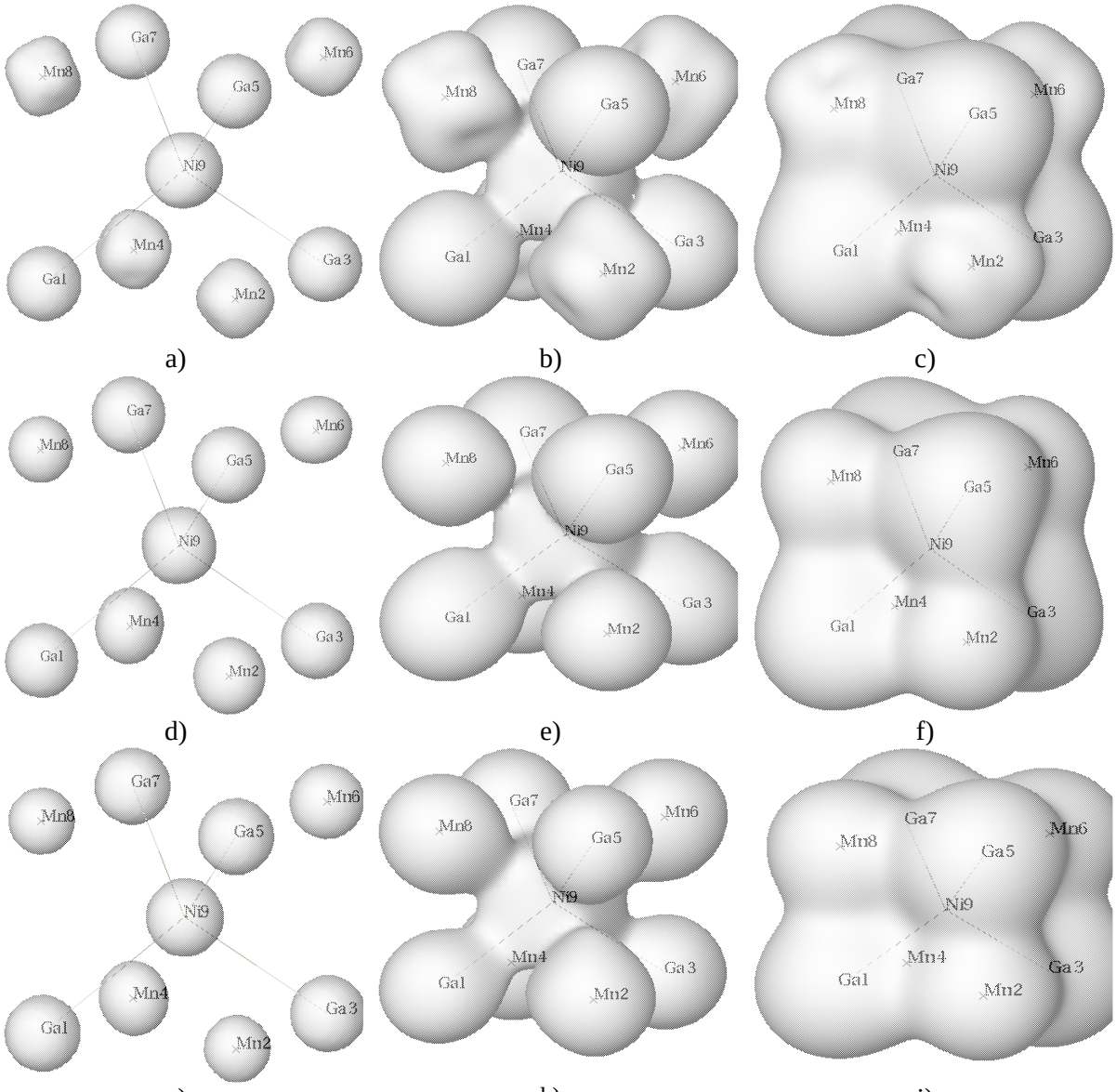

Fig. 6. Isosurfaces of electron density ρ for $NiMm_4Ga_4$ cluster in septet state: a-c for ROHF calculation, d-f for UHF calculation, g-i for DFT calculation a,d,g – isosurface corresponds to lg ρ=0; b,e,h – isosurface corresponds to lg ρ=-1.5 in atomic units; c,f,i - isosurface corresponds to lg ρ=-2.

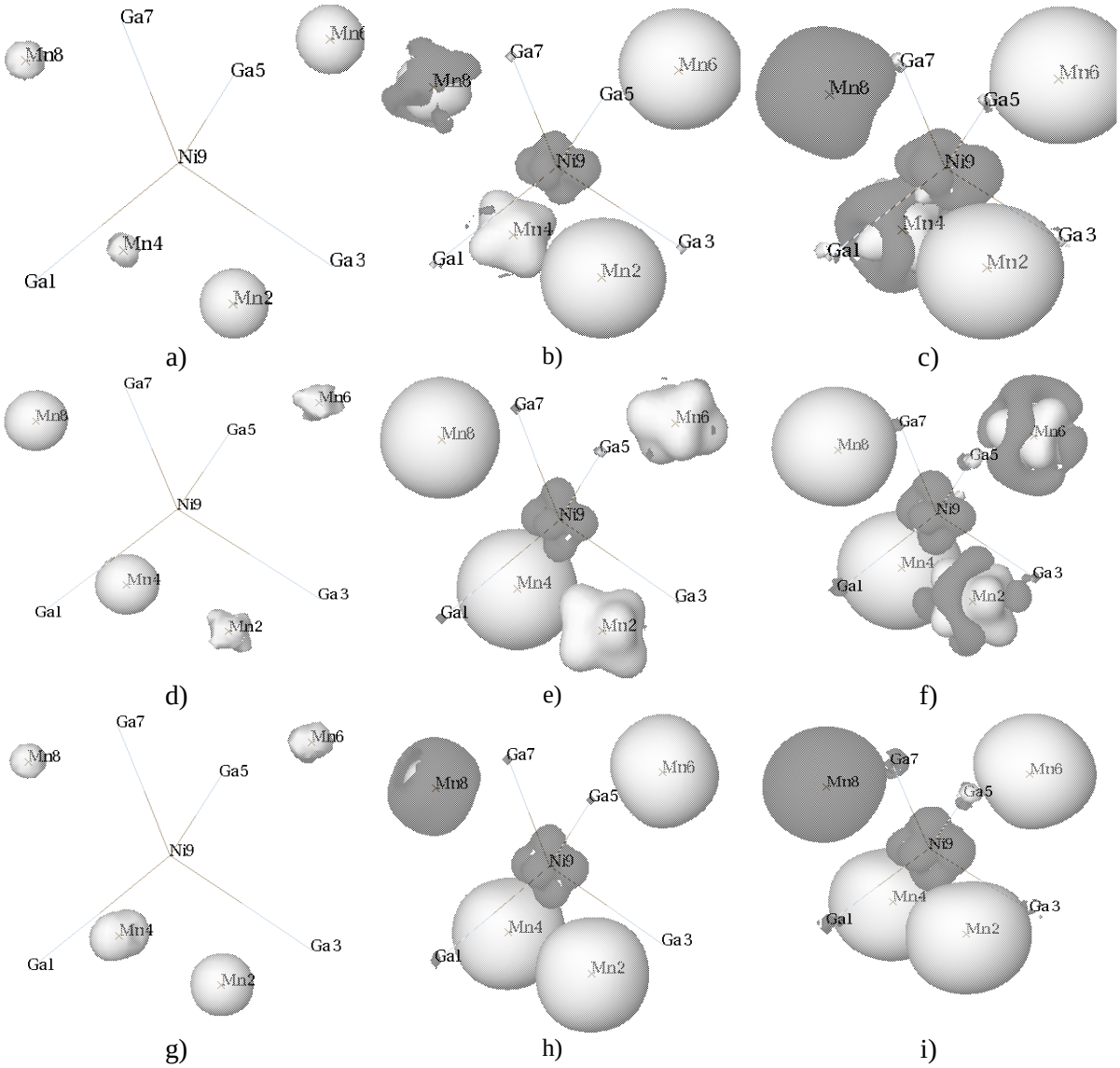

Fig. 7. Isosurfaces of electron spin density ρ_S for $NiMm_4Ga_4$ cluster from DFT calculations: a-c for triplet state, d-f for quintet state, g-i for septet state; a,d,g – isosurface corresponds to $lg|\rho_S|=0$; b,e,h – isosurface corresponds to $lg|\rho_S|=-1.5$ in atomic units; c,f,i - isosurface corresponds to $lg|\rho_S|=-2$.

5. Conclusions

The results obtained indicate that thermal stabilisation is important in stabilisation of martensitic structure. The incidental effect is there the appearance of microcracks along the interface. Properties of the system were investigated both experimentally and by ab initio simulation in NWChem package. Compatibility of Ni2MnGa crystal structure and cell parameters with semiconductors and also presence of spin-polarization of carriers opens up possibilities of the Ni2MnGa use in semiconductor spintronics.

Acknowledgments

The work was partially supported by EC FP7 project BalticGrid-II, grant 223807, Belarussian state program “Nanotech 2006-2010”, grant 4.19, and the “Triada” Scientific Technical Program of the Belarus-Russia Union State, grant ПА 2.7. Authors want to express gratitude to EMSL for providing them with NWChem and ECCE packages.

References

[1] V.A. Chernenko, E. Cesari, V.V. Kokorin, I.N. Vitenko // *Scripta Metallurgica et Materialia* **33** (1995) 1239.
[2] V. Martynov, V. Kokorin // *J. Phys. III (France)* **2** (1996) 739.
[3] T. Breczko, V. Nelayev, K. Dovzhik, M. Najbuk and M. Bramowicz // *Proceedings of NDTCS* **13** (2008) 89.
[4] A.A. Likhachev and K. Ullakko // *Phys. Letters* **A275** (2000) 142.
[5] Q. Pan and R.D. James // *J. Appl. Phys*. **87** (2000) 4702.
[6] Y. Murakami, D. Shindo, K. Oikawa // *Appl. Phys. Lett*. **82** (2003) 3695.
[7] Y. Kishi, C. Craciunescu, M. Sato, T. Okazaki, Y. Furuya, M. Wuttig // *J. Magn. Magn. Mater*. **262** (2003) L186.
[8] O.M. Korpusov, R.M. Grechishkin, V.V. Koledov, V.V. Khovailo, T. Takagi, V.G. Shavrov, // *J. Magn. Magn. Mater*. **272-276** (2004) 2035.
[9] V.A. Chernenko, A.R. Lopez, M. Kohl, M. Ohtsuka, I. Orue, J.M. Barandiaran // *J. Phys.: Condens. Matter* **17** (2005) 5215.
[10] T. Breczko, M. Bramowicz // Techn. Sci. No 7, 2004.
[11] E.J. Bylaska, W.A. de Jong, N. Govind, K. Kowalski, T. P. Straatsma, M. Valiev, D. Wang, E. Apra, T.L. Windus, J. Hammond, P. Nichols, S. Hirata, M.T. Hackler, Y. Zhao, P.-D. Fan, R.J. Harrison, M. Dupuis, D.M.A. Smith, J. Nieplocha, V. Tipparaju, M.Krishnan, Q. Wu, T. van Voorhis, A. A. Auer, M. Nooijen, E. Brown, G. Cisneros, G.I. Fann, H. Fruchtl, J. Garza, K. Hirao, R. Kendall, J.A. Nichols, K. Tsemekhman, K. Wolinski, J. Anchell, D. Bernholdt, P. Borowski, T.Clark, D. Clerc, H. Dachsel, M. Deegan, K.Dyall, D. Elwood, E. Glendening, M. Gutowski, A. Hess, J. Jaffe, B. Johnson, J. Ju, R. Kobayashi, R. Kutteh, Z. Lin, R.Littlefield, X. Long, B. Meng, T. Nakajima, S. Niu, L. Pollack, M. Rosing, G. Sandrone, M. Stave, H. Taylor, G. Thomas, J. van Lenthe, A. Wong, Z. Zhang, *NWChem, A Computational Chemistry Package for Parallel Computers, Version 5.1*. Richland, Washington 99352-0999: Pacific Northwest National Laboratory, 2007.
[12] T.M. Breczko, V. Nelayev, K. Dovzhik and M. Najbuk // *Proc. of SPIE* Vol.**7377** (2008) 7377OK-19**.**
[13] H. Rumpf, C. Craciunescu, J. Feydt, A. Gilles1, M. Wuttig, E. Quandt, *// Mat. Res. Soc. Symp. Proc*. **785** (2004) D7.2.1.
[14] V.V. Martynov, V.V. Kokorin // *J. Phys. III (France)* **2** (1992) 739.
[15] A.A.Vasil'ev, V. D. Buchel'nikov, T. Takagi, V.V. Khovailo, E.I. Estrin // *Phys. Usp.* **46** (2003) 559.
[16] S. Fujii, S. Ishida, and S. Asano // *J. Phys. Soc. Japan* **64** (1995) 185.
[17] K.E.H.M. Hanssen, P.E. Mijnarends, L.P.L.M. Rabou, and K.H.J. Buschow // *Phys. Rev*. **B42** (1990) 1533.
[18] S. Ishida, T. Masaki, S. Fujii, and S. Asano // *Physica* **B 245** (1998) 1.
[19] S. Ishida, S. Fujii, H. Nagayoshi, and S. Asano // *Physica* **B254** (1998) 157; Galanakis // *J. Phys.: Condens. Matter* **14** (2002) 6329.
[20] G.A. de Wijs and R.A. de Groot // Phys. Rev. **B64** (2001) 020402.